# REPORT DOCUMENTATION PAGE

Form Approved
OMB No. 0704-0188



| 1. AGENCY USE ONLY (Leave blank) | 2. REPORT DATE | 3. REPORT TYPE AND DATES COVERED |
|---|---|---|
| | 5/7/97 | Final Report 1/1/90-9/30/96 |

**4. TITLE AND SUBTITLE**
A Study of Oceanic Subduction using Tritium-Helium Dating

**5. FUNDING NUMBERS**
N00014-90-J-1387

**6. AUTHOR(S)**
Dr. William J. Jenkins

**7. PERFORMING ORGANIZATION NAME(S) AND ADDRESS(ES)**
Department of Marine Chemistry and Geochemistry
MS #25
Woods Hole Oceanographic Institution
Woods Hole, MA 02543

**8. PERFORMING ORGANIZATION REPORT NUMBER**

**9. SPONSORING/MONITORING AGENCY NAME(S) AND ADDRESS(ES)**
Scientific Officer Code: 322
Ron Tipper
Office of Naval Research
800 North Quincy Street
Arlington, VA 22217-5000

**10. SPONSORING/MONITORING AGENCY REPORT NUMBER**

**11. SUPPLEMENTARY NOTES**

**12a. DISTRIBUTION/AVAILABILITY STATEMENT**
Approved for public release; distribution is unlimited

**12b. DISTRIBUTION CODE**

**13. ABSTRACT** *(Maximum 200 words)*

Tritium and $^3$He measurements were made on samples taken at over 200 stations during the period 1991-1993 in the Subduction Area. Combining these data with salinity, oxygen and geostrophy we can compute isopycnal diffusivities, oxygen consumption rates, and absolute velocities. The reference level velocities are determined to an accuracy of 1mm/s. A classic absolute velocity spiral is seen. The depth variation of computed vertical velocities is consistent with vorticity conservation, and extrapolates to within errors of surface ekman pumping and subduction rates. Isopycnal diffusivities are approximately 1200 $m^2/s$ at a depth of 300m, and decrease gradually downward.

The oxygen utilization rates (OURs) determined by the oxygen equations show an exponentially decreasing magnitude with depth. On the shallowest horizons. Vertical integration of OUR yields a net water column oxygen demand of 4 $mol(O_2)/m^2/y$, which corresponds to an export production of 2.5 $mol/m^2/y$ carbon. I present a simple scheme to show how to relate the $^3$H-$^3$He age to the advective age, and after correcting for vortex stretching, compute the subduction rate as a function of depth. The shallowest horizon has a subduction rate indistinguishable from climatological ekman pumping rates, but gradually exceeds the projected rates with depth. The difference may be attributed to the increasing importance of buoyancy forced subduction at higher latitudes.

| 14. SUBJECT TERMS | | | 15. NUMBER OF PAGES 14 |
|---|---|---|---|
| | | | 16. PRICE CODE |
| 17. SECURITY CLASSIFICATION OF REPORT | 18. SECURITY CLASSIFICATION OF THIS PAGE | 19. SECURITY CLASSIFICATION OF ABSTRACT | 20. LIMITATION OF ABSTRACT UL |

NSN 7540-01-280-5500

Standard Form 298 (Rev. 2-89)
Prescribed by ANSI Std. Z39-18
298-102

19970512 094

Submitted to The Office Of Naval Research
April 25, 1997

# Final Technical Report for N00014-90-J-1387: A Study of Oceanic Subduction using Tritium-Helium Dating

W.J. Jenkins
Woods Hole Oceanographic Institution
Woods Hole MA.

## Abstract

*In the Subduction Area of the eastern subtropical North Atlantic, tritium and $^3$He measurements were made on samples taken at over 200 stations during the period 1991-1993. Combining these data with salinity, oxygen and geostrophy we can compute isopycnal diffusivities, oxygen consumption rates, and absolute velocities. The reference level velocities are determined almost solely by the $^3$H-$^3$He age equations and to an accuracy of better than 1mm/s. A classic absolute velocity spiral is seen. The depth variation of computed vertical velocities is consistent with vorticity conservation, and extrapolates to within errors of surface ekman pumping and subduction rates. Isopycnal diffusivities are largely constrained by the salinity equations, and are approximately 1200 m$^2$/s at a depth of 300m, and decrease gradually downward. Diffusivities apparently decrease toward the surface, likely an artifact of either diapycnal mixing or proximity to the outcrop, where unsteadiness may be important..*

*The oxygen utilization rates (OURs) determined by the oxygen equations show an exponentially decreasing magnitude with depth. On the shallowest horizons, estimated rates based on a simple regression between A.O.U. and $^3$H-$^3$He age on isopycnals agree well with the more complete analysis done here, but diverge toward higher values in the deeper strata. This is an artifact of isopycnal mixing combined with regionally concave A.O.U. fields masquerading as consumption in the simplistic analysis. Vertical integration of OUR yields a net water column oxygen demand of 4.1±0.8 mol($O_2$)/m$^2$/y, which corresponds to an export production of 2.5±0.5 mol/m$^2$/y carbon.*

*If the $^3$H-$^3$He age is a true representation of the advective age of fluid parcels, then its inverse gradient for a given isopycnal may be used to compute the subduction velocity projected back to its outcrop. I present a simple scheme to show how to relate the $^3$H-$^3$He age to the advective age, and after correcting for vortex stretching, compute the subduction rate as a function of depth. The shallowest horizon has a subduction rate indistinguishable from climatological ekman pumping rates, but gradually exceeds the projected rates with depth. The difference may be attributed to the increasing importance of buoyancy forced subduction at higher latitudes.*

## 1. Introduction

Tritium ($^3$H) was produced as a result of atmospheric nuclear weapons testing in the late 1950s and early 1960s, entering the oceans predominantly *via* precipitation and water vapor exchange. It is valuable to observe tritium's entry into and movement through the hydrosphere as a dye-like tracer, but its main utility in studying thermocline ventilation comes from the fact that it decays to a stable, inert tracer: $^3$He. Rather than looking at the distributions of $^3$H and $^3$He separately, it is useful to combine them to compute a "tritium-helium age". Inasmuch as excess (tritiugenic) $^3$He is lost to the atmosphere from the surface layer, and accumulates once a fluid parcel leaves the sea surface, the two tracers can be combined to compute a $^3$H-$^3$He age that is a measure of the time elapsed since a water parcel was at the sea surface,

$$\tau = \lambda^{-1}\log\left(1 + \frac{^3\mathrm{He}}{^3\mathrm{H}}\right).$$

With typical northern hemispheric upper-water tritium concentrations and present measurement technology, times as short as two or three months or as long as a few decades can, in principle, be detected on individual samples. Such time-scales are ideal for the study of oceanic subduction, thermocline ventilation and biological productivity.

The purpose of this work was to study subduction in the eastern subtropical North Atlantic, and its role

in the ventilation of the main thermocline. The work involved obtaining and analyzing tritium and helium-3 samples from three cruises in the Subduction Area, and interpreting the results in the context of

- what are the relative contributions of frontal *vs.* distributed subduction?
- can we see the "smoking gun" of subduction?
- what are the rates of subduction as a function of density class, and are they consistent with ekman pumping rates?
- what is the circulation of the subducted waters?
- what are the oxygen consumption rates in these waters?
- how does the granularity of tracer distributions evolve downstream (does it grow or erode)?

and to demonstrate that these observations can yield quantitative information about mixing, dilution, ventilation and circulation. We accomplished all of these goals with considerable success. The highlight of this work is that we were able to obtain estimates of subduction rates for the area, and were able to determine area averaged *absolute* velocities to an accuracy of 0.1 cm/s. In addition, we have quantitative estimates of vertical velocities, isopycnal diffusivities, and oxygen consumption rates.

## 2. Mixing and the Tritium-Helium Age

Ideally, one would like to interpret the tritium-helium age in the simplest possible context: the gradient in the age is inversely proportional to the velocity on a given surface. This might be the case in a simple, linear flow with no mixing, but the tritium-helium age must obey the conservation equation (Jenkins, 1987)

$$\frac{\partial \tau}{\partial t} = \nabla(\kappa \nabla \tau) - u \bullet \nabla \tau + 1 + \kappa\left(\frac{\nabla \zeta}{\zeta} + \frac{\nabla \vartheta}{\vartheta}\right) \bullet \nabla \tau \qquad (1)$$

where $\vartheta$ is $^3H$, $\zeta$ is the sum of $^3H$ and $^3He$, and $\kappa$ is the turbulent diffusivity. This equation resembles that for "A", the *ideal age tracer*, which obeys

$$0 = \nabla(\kappa \nabla A) - u \bullet \nabla A + 1 \qquad (2)$$

except for the unsteady term on the LHS, and the "pseudo-advective" term on the far right. The latter term may be regarded as pseudo-advective since it appears as a scalar product with the age gradient. In younger waters (less than a decade old) the tritium distributions are homogenized, so the resultant gradients (and hence this and the unsteady term) are small. In older waters the general sense of the $\vartheta$ and $\zeta$ gradients are negative downstream, yielding an apparent increase in "velocity" due to mixing non-linearities. The magnitudes of these terms, in relation to the others, are significant but manageable (see Jenkins, 1987 and below). The important point to note, however, is that these terms, provided that $\kappa$ is known, are all measurable quantities, and hence can be accounted for.

It was expected that the Subduction Area, in the eastern subtropical gyre, would be a place were mixing effects on the age were small. This can be seen with a simple, two-dimensional gyre simulation such as the one depicted in figure 1. In this simulation, velocities were characteristically order 1 cm/s in the eastern part of the gyre (consistent with the beta-spiral results of Armi and Stommel, 1983) and an isopycnal diffusivity of 1000 $m^2/s$ was used. The entry of tritium and the generation of $^3He$ on an isopycnal surface in an idealized Stommel-type gyre were simulated as a function of time and "forced" using an extended version of the Dreisigacker-Roether (1979) surface water tritium history, and the tritium-helium age computed from the tritium and $^3He$ concentrations. The isopycnal had an outcrop (the grey area) where some of the streamlines (indicated by the dashed lines in the figure) intersected the sea surface. Note that there are two types of streamlines in model. *Open streamlines,* which enter the surface directly from the outcrop region represent fluid that is subducted directly onto the isopycnal, and hence may referred to as the "directly ventilated region". On the other hand, *closed streamlines* which do not intersect the outcrop, represent recirculated waters within the gyre, whose ventilation must be accomplished by cross-streamline mixing. These streamlines form an "unventilated pool region" in the western part of the gyre. The upper panel in figure 1 shows the tritium-helium age distribution in the early 1990s on this isopycnal. Note that the two regions have a characteristic relationship between the *isochrons* (contours of constant tritium-helium age) and streamlines: in the directly ventilated region, the isochrons are mostly perpendicular to the streamlines, whereas in the unventilated pool, they are mostly parallel. The former is a signature of an advectively dominated system, while the latter signifies a

mixing dominated regime (*i.e.*, to enter a streamline, tritium must diffuse across streamlines).

The lower panel in figure 1 shows the influence of mixing on the tritium-helium age, by showing the ratio of the tritium-helium age to the "ideal tracer age" defined by equation 2. One can readily see that in the directly ventilated region in the eastern portion of the gyre, *i.e.*, the Subduction Area, the ratio is very nearly one, indicating that the tritium-helium age is behaving much like an ideal age tracer. This is consistent with arguments advanced earlier (Jenkins, 1987). In the unventilated pool region in the west, however, there exist substantial differences between the tritium-helium and ideal tracer ages, a signature of mixing. The tritium-$^3$He age is generally depressed relative to the ideal tracer age. Note how iso-ratio lines tend to be parallel to streamlines in the unventilated pool region. In general, though, the tritium-$^3$He/ideal age ratio is within 10% of 1 in the eastern portion of the gyre. The conclusion to be drawn from this simple modeling exercise, then, is that the tritium-helium age tracer will be dominated by advective effects, but some caution must be used to account for the influence of recirculated waters. In the analysis which follows, this influence is properly accounted for.

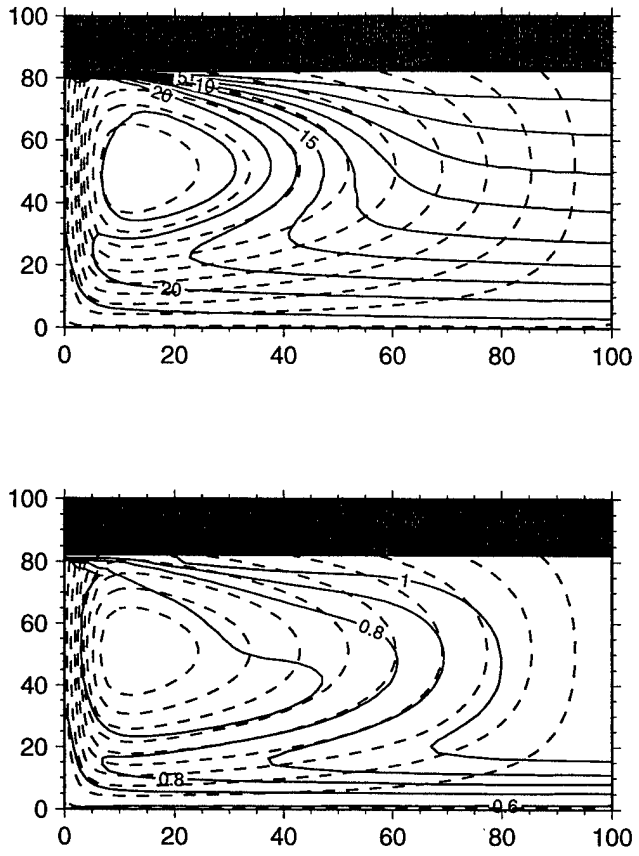


Figure 1: Simulation of tritium penetration and the tritium-helium age in an idealized Stommel gyre. Isochrons are solid lines (upper panel) while streamlines are dashed. Ratio of tritium-$^3$He age to ideal age in lower panel.

## 3. Tritium-Helium Sampling and Measurement

The Subduction Area is in the eastern subtropical North Atlantic, an area expected to resemble the directly ventilated portion of the thermocline in the simple gyre model described above. Here, one would expect the $^3$H-$^3$He age to be a more accurate measure of the ventilation age. As part of this multidisciplinary, multi-institutional Advanced Research Initiative by the Office of Naval Research, we measured tritium and $^3$He at a large number of locations and depths in the eastern subtropical North Atlantic, between approximately 40 and 18°W, 18 and 38°N from May 1991 through May 1993 (figure 2). Two cruises, in May, 1991 and May 1993 were focused on mesoscale tracer variability, and appear in the map as "L" shaped arrays. The largest scale coverage was accomplished during two cruises in October-November, 1992. We also obtained additional samples during December, 1992 taken for us by T. Joyce.

Samples were obtained from Niskin bottles during standard CTD-Rosette casts, and transferred to 90 cc valved, stainless steel cylinders. Dissolved gases were subsequently extracted on shipboard using our newly developed at-sea extraction system into aluminosilicate glass ampoules (Lott et al, 1997). On return to the shore-based laboratory, the gases were purified and separated cryogenically and helium isotopes measured using a statically operated, dual collecting, $\pi/2$ magnetic deflection mass spectrometer (Lott and Jenkins, 1984), while neon concentrations were determined using an ancillary quadrupole mass spectrometer. The measurement standards used were volumetric aliquots of marine air at known pressure, temperature and relative humidity, and the results were corrected for a small dependence of the measured helium isotopic ratio on sample size. The running air standard was repeatedly compared to external air standards to ensure consistency and accuracy The isotope measurements are reported as an isotope ratio

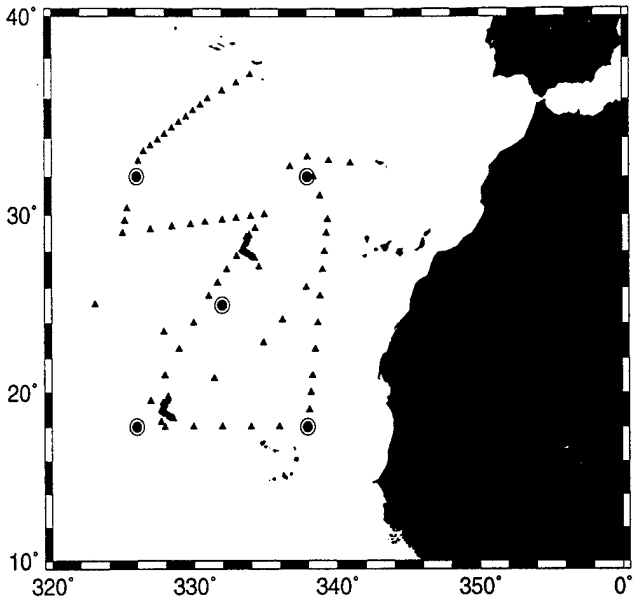


Figure 2: Tritium-$^3$He station locations (filled triangles) for the Subduction Experiment. The "L" shaped features are densely sampled mesoscale resolving patterns. The solid circles designate the position of current meter and meteorological moorings.

anomaly of the unknown (x) relative to the atmospheric standard (A) in per mil.

$$\delta(^3\mathrm{He}) = \left( \frac{(^3\mathrm{He}/^4\mathrm{He})_x}{(^3\mathrm{He}/^4\mathrm{He})_A} - 1 \right) \times 1000$$

and are accurate to better than 1.5 permil as determined by a combination of standard reproducibility and comparison of replicate samples.

Concentrations of helium and neon, calculated using ion current manometry, again relative to the atmospheric standard, were determined to better than 0.2%. Helium saturation anomalies are computed using the solubility data of Weiss (1970) according to

$$\Delta\mathrm{He} = \left( \frac{C}{C^*} - 1 \right) \times 100\%$$

and similarly for Ne.

Tritium samples were also degassed on shipboardand stored *in vacuo* in 200 cc aluminosilicate glass flasks. These were returned to the laboratory and stored for approximately one year for determination of tritium by the $^3$He regrowth technique (Clarke *et al,* 1976; Jenkins *et al,* 1983). The tritium was typically measured to an accuracy of 0.02 T.U.

## 4. Results

Figure 3 is a map of $^3$H-$^3$He age on two isopycnal surfaces in the area. The shallower surface ($\sigma_\theta$=26.4 kg/m$^3$) outcrops in this area during the winter, while the deeper ($\sigma_\theta$=26.6 kg/m$^3$) outcrops further north. The shallower surface is clearly tainted with freshly subducted water, as evidenced by the patch of water less than a year old on the eastern portion of the surface. The $^3$H-$^3$He age increases to the west and the south, as would generally be expected for a southwestward flow in this portion of the gyre: the $^3$H-$^3$He age should increase

downstream. The deeper surface is characterized by both a greater average $^3$H-$^3$He age and an apparently more pronounced age gradient. The "isochrons" (contours of constant $^3$H-$^3$He age) have organized themselves in a more orderly northwest-southeast orientation. Note that there is no evidence of young (less than one year old) water on this surface, and that the youngest ages are found on the northernmost and shallowest portion of the isopycnal in the vicinity of the Azores Front. This suggests that the Front may play a role in ventilation of this isopycnal in the region, possibly by cross-frontal mixing and lateral induction processes (*e.g.*, see Qiu and Huang, 1995).

If the distributions of tritium-helium age, salinity, and oxygen are known in three dimensions over a portion of the subtropical gyre, it is possible to combine them with the field of mass (*via* the geostrophic relation) to compute absolute velocities and isopycnal diffusivities, as well as oxygen consumption rates. This is done by first computing the geostrophic velocity field relative to an arbitrary reference level (which need not be at rest), and constructing a series of conservation equations for those properties on each isopycnal. The "known" quantities, which include the geostrophic velocities, observed gradients, time derivatives, *etc.* are substituted into the equations, and organized so that the unknowns (diffusivities, consumption rates, and reference level velocities) are on the left-hand side. One thus obtains an over-determined system of equations that can be solved in a least-squares sense for the unknown variables.

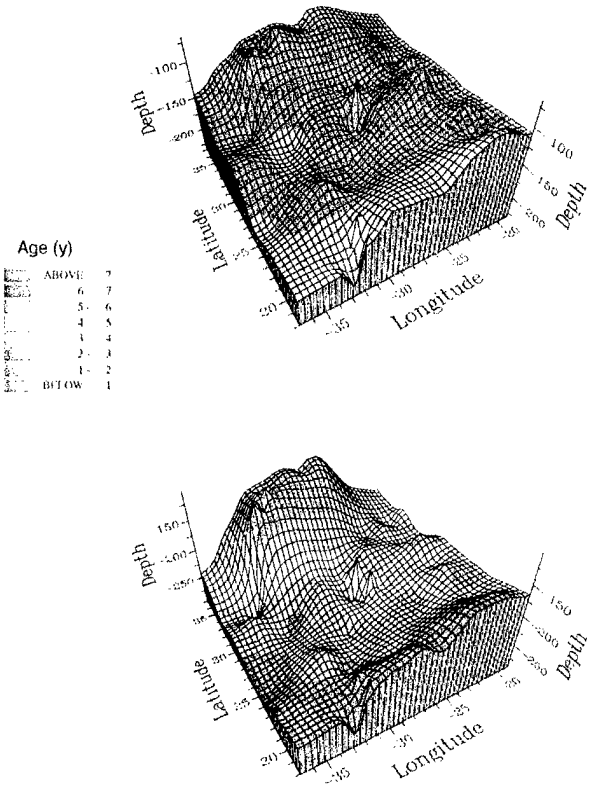


Figure 3: Tritium-$^3$He age distributions on the 26.4 (upper) and 26.6 (lower) kg/m$^3$ isopycnal surfaces *vs.* depth..

Samples were taken at over 200 stations during a series of four cruises between May 1991 and May 1993. Measurement precisions for $^3$H and $^3$He were 0.02 and 0.03 TU respectively, resulting in a $^3$H-$^3$He age resolution of approximately 0.25 years for an individual measurement and 0.08 years from systematic uncertainties. The data were interpolated onto isopycnal surfaces (in 0.1 kg/m$^3$ increments from $\sigma_\theta$ = 26.4 to 27.1 kg/m$^3$) using a simple local spline routine on a station-by-station basis. Estimates of large scale averages, isopycnal gradients and laplacians for properties, along with attendant statistical uncertainties, are obtained by doing a biquadratic fit of the interpolated data on isopycnals (solving the normal equations using SVD). Since in general the station spacing is comparable to decorrelation scale of the tracers (100-150km), the statistical uncertainties associated with the parametric determinations is a reasonable measure of uncertainties in the quantities of interest. Laplacians obtained from these fits are thus averaged over the whole region (an approximately 1500 km square), but the gradients, evaluated at the center of the region, are a more local average (perhaps of order 500 km square).

Time derivatives for the $^3$H-$^3$He age are determined by mapping the $^3$H-$^3$He age on the same set of isopycnals for the Subduction Experiment data and for the TTO/NATS (1981) data separately, and interpolating to a common location (25° N, 28° W). The age differences between the two data sets are then divided by the time differences to obtain the average time derivative in $\tau$ as a function of $\sigma_\theta$. Statistics of the fits suggest an uncertainty in this estimate ranging from 0.02 to 0.06, which should be compared to the age tendency term of 1. The geostrophic calculations were performed using the Levitus (1994) hydrographic data-base interpolated to isopycnal surfaces. The geostrophic velocities were computed at the center of the region for each isopycnal from the thermal wind equation, with gradients computed using biquartic fits to the climatological data. Climatological data were used to compute the streamfunction rather than the individual station data to avoid transient eddy variability in the density field. Any arbitrary reference level may be chosen, and here I

used the 1000db surface. For the eight isopycnal surfaces in this study ($\sigma_\theta$ = 26.4 - 27.1 kg/m$^3$) one obtains a set of 24 equations, patterned after:

$$\tau_x u_b + \tau_y v_b - \left(\nabla^2\tau + \left(\frac{\nabla\vartheta}{\vartheta} + \frac{\nabla\zeta}{\zeta}\right) \bullet \nabla\tau\right)\kappa_i = 1 - \frac{\partial\tau}{\partial t} - \tau_x u_g - \tau_y v_g \qquad (3)$$

for the $^3$H-$^3$He age ($\tau$),

$$S_x u_b + S_y v_b - (\nabla^2 S)\kappa_i = -S_x u_g - S_y v_g \qquad (4)$$

for salinity (S), and

$$O_x u_b + O_y v_b - (\nabla^2 O)\kappa_i - J_i = -O_x u_g - O_y v_g \qquad (5)$$

for dissolved oxygen (O). Here *u* and *v* are the zonal and meridional velocities, and the subscripts b and g correspond to reference level and geostrophic components respectively. $\kappa_i$ and $J_i$ are the diffusivities and zero order oxygen utilization rates, which are assumed to be a function of depth, and hence isopycnal. Thus, one has 24 equations in 18 unknowns, which may be solved by least squares. Prior to solution, the equations were scaled (row normalized) by dividing by measurement uncertainties. The solutions (particularly the reference velocities) were insensitive to the precise scaling factors.

### 4.1 Absolute velocities and Diffusivities

The solution of the reference level velocity components is dominated by the $^3$H-$^3$He age ($\tau$) equations, because the $^3$H-$^3$He age distributions, especially on the shallowest isopycnals, are dominated by advective effects. Further, the $\tau$ equations prove to be linearly independent for $u_b$ and $v_b$ since the $\tau$ gradient vector rotates significantly relative to the velocity vector with increasing depth. Notably, the age equations are mutually consistent within measurement errors. I can therefore solve for the reference level velocities, and hence compute the absolute velocities for each of the isopycnal surfaces. The statistical uncertainty in the magnitude of the reference level velocity component thus estimated is 0.09 cm/s. This may then be recombined with the geostrophic velocities, providing a measure of the absolute velocity to an accuracy of 0.10 to 0.12 cm/s for individual isopycnal surfaces. The absolute velocities, along with estimated uncertainties are plotted in figure 4. The velocity spiral observed is consistent in direction with that expected from a $\beta$-spiral calculation (*cf.* Armi and Stommel, 1983) but opposite to that originally obtained using a more simplistic treatment of $^3$H-$^3$He age distributions (Jenkins, 1987). The velocities are roughly consistent in magnitude with the $\beta$-spiral velocities (Armi and Stommel, 1983) obtained nearby for comparable depth ranges. These velocities also agree with the shallow Bobber Float displacements (Jim Price, priv. comm.) but a detailed comparison is made difficult by the fact that the Floats track isothermal surfaces that diverge from isopycnals in this area.

The isopycnal diffusivities, shown in figure 5 (left panel), are largely determined by the salinity equations. Uncertainties in the $\kappa$ estimates are obtained by error propagation calculations using uncertainties in the salinity gradients and laplacians, and in velocities. Given the relatively small size of the mixing terms in the $^3$H-$^3$He age equations (figure 5, right panel), uncertainties in $\kappa$ play a very small role in the determination of $u_b$ and $v_b$. The age laplacian term becomes increasingly important with depth due to the combined effects of deceleration and the rotation of the planetary scale $^3$H-$^3$He age gradient relative to streamlines.

The interesting feature, not discussed in the earlier $\beta$-Triangle analysis (*Jenkins, 1987*) is the size of the unsteady term. This term is smallest on the shallowest surfaces whose mean "age" is short compared to the time elapsed since the major tritium input, but is larger for the deeper isopycnals whose ages are comparable to that time frame. That is, the deeper isopycnals are still undergoing significant tritium and $\zeta$ redistribution, and hence $^3$H-$^3$He age evolution. The unsteady term thus becomes significant on the deeper isopycnals, and must be accounted for.

The oxygen equations do not influence the estimated diffusivities ("turning down" the weighting of the oxygen equations by orders of magnitude does not change the estimated $\kappa$). The isopycnal diffusivities calculated are smaller on the shallowest isopycnal and tend to increase weakly downward to approximately 1200 m$^2$/s at 300 m depth; and decrease very gradually below. Overall these diffusivity estimates are lower than that obtained for the Sargasso Sea (Jenkins, 1991), which is consistent with large scale patterns of eddy ki-

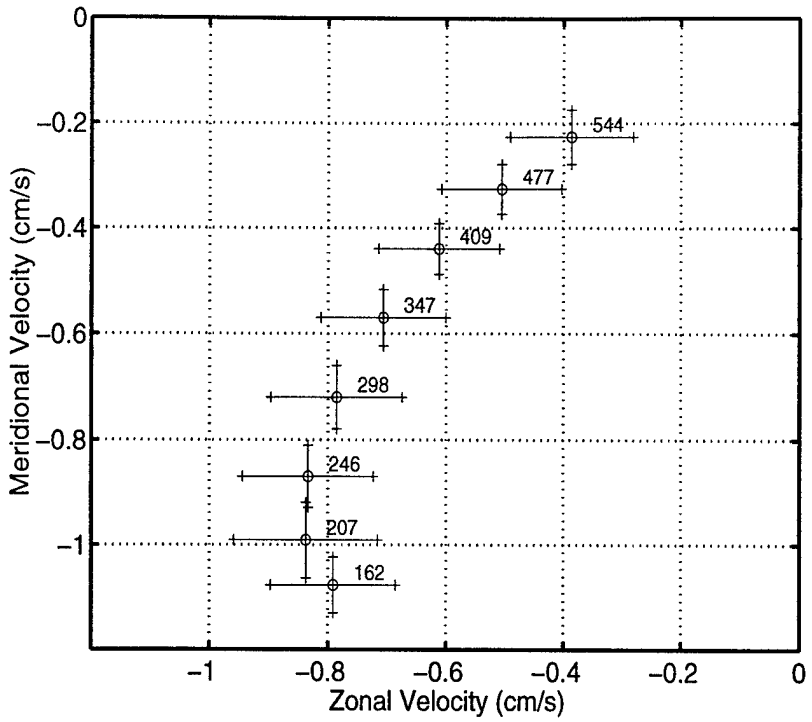


Figure 4: The absolute velocity spiral computed from the tracer balance equations.

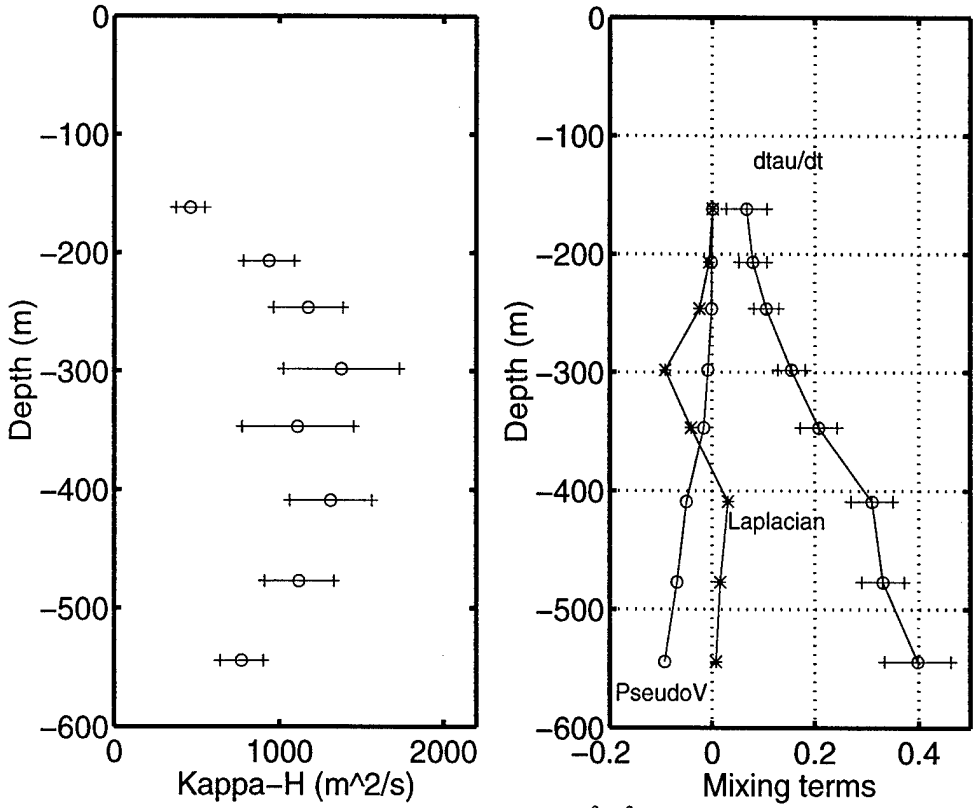


Figure 5: Computed isopycnal mixing coefficients (left panel) and $^{3}H$-$^{3}He$ age mixing and tendency terms (right panel) for the range of isopycnals from 26.4 to 27.1 kg/m$^3$.

netic energy (*op cit.*). These values are slightly larger than, but roughly consistent overall with values obtained from β-spiral calculations (Armi and Stommel, 1983; Jenkins, 1987) and inversions of climatological data (*e.g.*, Olbers *et al.*, 1985; Hogg, 1987). The deeper decrease in isopycnal diffusivity is consistent with intuition based on the reduction of velocities (and shear) with depth.

The decrease in isopycnal diffusivity toward the surface is unexpected, since eddy kinetic energy is roughly constant with depth, or tends to increase upward (*e.g.*, Muller and Siedler, 1992). This decrease in $\kappa_i$ toward the surface suggests the existence of unaccounted-for terms in the salinity equation (since it dominates the diffusivity determination) which increase upward in importance. The two primary candidates are diapycnal diffusion of salinity ($\kappa_i S_{zz}$) and a possible unsteady term ($S_t$). The former might arise from significant vertical curvature of salinity profiles, coupled with an upward increase in diapycnic mixing rates. This can be roughly evaluated by computing the magnitude of diapycnal mixing rate that would be required to become significant relative to the advective flux divergence terms in equation 4. Using a number of CTD profiles from the central region of the Subduction area, I estimate the average vertical curvature in salinity at the depth of the $\sigma_\theta = 26.4$ kg/m$^3$ surface to be approximately $5\times10^{-5}$ PSU/m$^2$. Computing the isopycnal advective salinity divergence to be approximately $5\times10^{-8}$ PSU/s using the velocities I have obtained coupled with the salinity gradients obtained from the biquadratic fits, I estimate that a diapycnal diffusivity of order $10^{-3}$ m$^2$/s would be required to make the terms equal. This value seems improbably large in light of recent determinations of diapycnal mixing rates within the main thermocline (Jenkins, 1980; Ledwell *et al.*, 1992) even with a fairly strong depth dependence.

Unsteadiness in the salinity balance equation is most likely significant on the shallowest surfaces, where insufficient time has passed for eddy mixing processes to achieve the erasure of surface patchiness subducted with the water mass and to reach a statistical equilibrium with the creation of variability by the work of eddies on large scale mean property gradients. The time required to achieve this may be crudely estimated from the isopycnal eddy mixing coefficient (estimated here to be of order 1000 m$^2$/s) and the tracer decorrelation length scale (estimated from tracer variability to be 100-150 km, see Jenkins, 1987; Joyce and Jenkins, 1993). This time scale is of order 1 year or less. Thus one would expect that on the shallowest isopycnal, especially those which outcrop locally and have ages of order 1-2 years or less, the unsteady term in the salinity equation may be significant, affecting the shallow estimates of isopycnal diffusivity. The age and oxygen equations, incidentally, are less likely to be affected due to the character of their surface boundary conditions (Jenkins, 1987; Doney and Jenkins, 1988).

One can also calculate the vertical velocity for each isopycnal from the absolute velocities using the relation $w = \vec{u} \bullet \nabla d$ where $d$ is the isopycnal depth (right panel of figure 6). In addition, one can compute the $w$ relationship with depth (the dashed line in figure 6, right panel) using the vorticity conservation equation $\beta v = f w_z$ and integrating upward from 500m using the tracer derived $v$. The computed $w$'s agree with the vorticity-derived curve within uncertainties (the error bars, and the dotted curves). They also generally agree with the vertical velocities obtained from the Bobber Float deployments (the * points, courtesy Jim Price). For reference, the local subduction rate obtained from the $^3$H-$^3$He age data (the vertical gradient of the $^3$H-$^3$He age may be argued to be the projected subduction rate for that density class) is plotted near 0 m depth in the figure (the open circle, see section 5). The tracer-computed $w$ curve appears to extrapolate to the $^3$H-$^3$He age estimated subduction rate, which also appears to be consistent with the local wind stress curl computed from the ECMWF gridded data (K. Moyer, priv. comm.) but a little smaller than climatological estimates (*e.g.*, Isemar and Hasse, 1987; Mayer and Weisberg, 1993).

## 4.2 Oxygen Consumption Rates

The distribution of oxygen on density surfaces correlates negatively with the $^3$H-$^3$He age, having high values in the north and northeast and lower values to the south. The downstream reduction of oxygen results largely from *in situ* consumption due to biological oxidation of sinking particulate matter and possibly dissolved organic carbon (*e.g.*, see Jenkins and Wallace, 1992). One is tempted to use the observed anticorellation between the $^3$H-$^3$He age and dissolved oxygen on isopycnal surfaces to directly estimate oxygen utilization rates (Jenkins, 1982, 1987). However, the proximity to the strong meridional gradient in oxygen observed roughly along 15 - 20° N means that one must account for mixing effects in the oxygen distributions. Such effects lead to the possibility of biases in such "determinations" of oxygen consumption rates, especially in deeper waters. Thus the approach here is to account fully for *all* processes affecting the dissolved

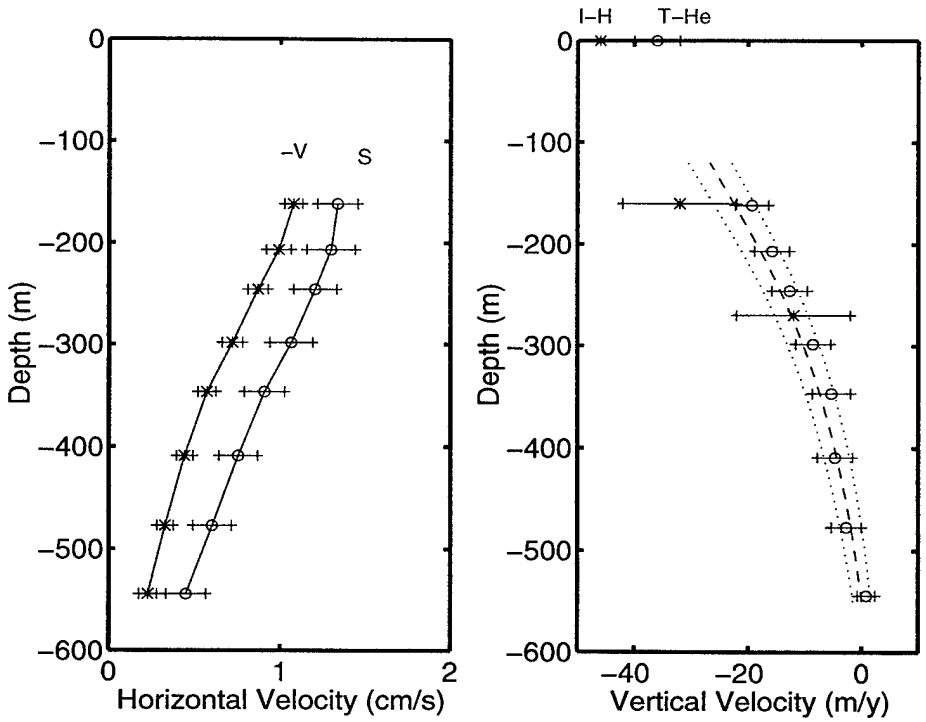


Figure 6: Meridional velocity component and velocity magnitude *vs.* depth (left panel) and computed vertical velocities (open circles, right panel). The curve is computed from the vorticity conservation equation, and the dotted lines constitute 1 standard error. The * are estimates based on isothermal float displacements (courtesy J. Price)

oxygen distribution.

Because they appear only once in each oxygen equation (equation 5), the apparent oxygen utilization rates ($J_i$) are not over-determined, but are uniquely solved for within the system of equations. Uncertainties in $J_i$ can be estimated by propagation of uncertainties in the velocities, diffusivities, and oxygen gradient and laplacian terms. The results are shown in figure 7 (left panel), along with uncertainties. For comparison, the estimated AOUR based on the slope of the regression between AOU and $^3$H-$^3$He age for each isopycnal surface is included in the plot (the solid line).

The oxygen utilization rates (OURs) in the shallowest layers are indistinguishable within uncertainties from both the regression based values, and earlier estimates (*op cit.*) in the β-triangle region. This is consistent with the relatively small diffusive flux divergence (figure 7, middle panel). The agreement is particularly remarkable in light of the significant directional difference between the oxygen and $^3$H-$^3$He age gradients (figure 7, right panel). Perhaps this is a further indication of the unimportance of mixing on these horizons.

OUR decreases in a quasi-exponential fashion with increasing depth, as would be expected from an attenuation of the available carbon with depth, but it does so more aggressively than the regression based results obtained both here and from the earlier β-triangle analyses. This increasing "bias" with depth in the regression technique arises from increasing prominence of the diffusive flux divergence with depth (see center panel of figure 7). Mixing driven by the latitudinally convex oxygen distribution, a feature imposed by the larger scale oxygen distributions, tends to masquerade as "consumption": as fluid parcels move down streamlines, oxygen is mixed away (largely to the south), decreasing oxygen concentrations in a fashion which resembles *in situ* consumption. Since the $^3$H-$^3$He age is not affected as much, this biases the regression estimates.

The role of mixing and the large scale gradients in the oxygen distributions in influencing the "downstream" change in oxygen also can be seen in the angle between the negative of the oxygen gradient and the velocity vector (figure 7, right panel). On the shallowest isopycnals, the large scale negative meridional gradient in oxygen is at about a 45° angle to the velocity, which is oriented west-southwestward. By 500 m, the velocity has rotated more westward, while the negative oxygen gradient has rotated due southward. As water flows southwestward, in addition to *in situ* consumption, oxygen is mixed away due to the convex nature of the large scale distribution, increasing the apparent utilization rate. Accounting for this process, as has been

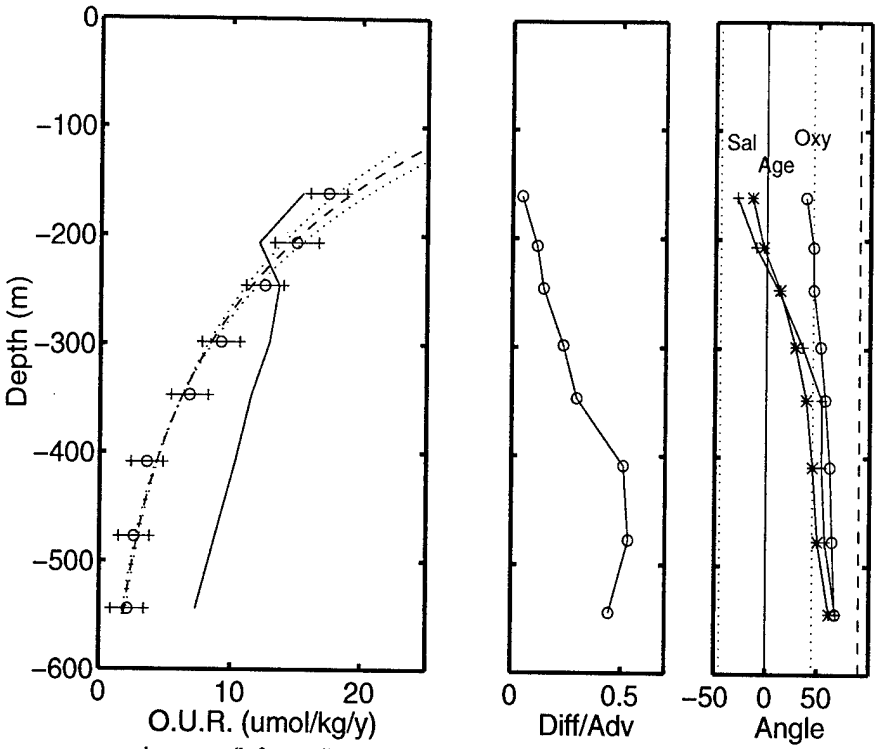


Figure 7: Oxygen consumption rates (left panel), the ratio of oxygen advective to diffusive divergence (middle panel) and the angle between property gradients and velocity vector (right panel) all *vs.* depth. Also in the left panel is the estimated oxygen utilization rate based on a linear correlation of AOU *vs.* $^3$H-$^3$He age for each isopycnal (solid line). The dashed line is the best fit exponential curve through $J_i$ and the dotted lines represent the uncertainties in the fit.

done here, provides us with a smaller, and more realistic consumption rate on the deeper isopycnals.

The OUR can be least squares fit to an exponential relationship with depth (the dashed line in the left panel of figure 7), with attendant uncertainties in the fit (dotted lines). The vertical scale height of the OUR decrease is 165 m. Using this relationship, one can integrate the OUR vertically between 120 m and 550 m to obtain the net oxygen demand per square meter. This integral is 4.1 ±0.8 mol($O_2$)/m$^2$/y. Using the revised $O_2$:C ratio of Takahashi *et al.* (1985), this implies an export production of 2.5±0.5 mol(C)/m$^2$/y. This rate is sensitive to the choice of the upper bound to the integration, but appears to be marginally smaller than estimated productivity for the Sargasso Sea (2.8 mol(C)/m$^2$/y, see Jenkins and Wallace, 1992), which is consistent with expectations based on the availability of nitrate. That is, the regions of deeper mode water formation in the northwestern gyre are areas of correspondingly higher nutrient supply and hence greater new production. However, it should be reiterated that the estimated integral oxygen demand (and hence productivity) based on this calculation is clearly different from the more incomplete treatments attempted earlier.

### 4.3 Consequences of the 3-dimensional and larger scale characteristics of distributions

There is a substantial difference in the oxygen utilization rate estimates between the calculations presented here and the less complete treatment of correlating AOU with $^3$H-$^3$He age (see the * profile in figure 7). The differences arise in part from the influence of the large scale mixing of properties associated, for example, with the confluence of waters of greatly differing origins. They also arise from the complex interplay among mixing, advection, and consumption, which must (and can) be fully accounted for.

The observed rotation of the age gradient with respect to the streamlines as a function of depth is also evident in the right hand panel of figure 7. On the shallower isopycnals, the two are virtually parallel, but proceeding down the water column, the age gradient rotates counterclockwise (southward) relative to the streamlines that in turn rotate westward with depth. This rotation in $^3$H-$^3$He age gradient of course results from the increasing dominance of the planetary scale distributions on the age distribution: the same "front" in properties seen in oxygen and salinity between 15 and 20° N is also seen in tritium and age: this is the

southern edge of the $\zeta$ lens embedded in the subtropical main thermocline. Also, the rotation is precisely why the system of equations used to solve for the reference level velocity is non-degenerate. The rotation of the age gradient with depth results in a smaller projected velocity $\vec{u} \bullet \nabla\tau$ on the deeper horizons, and hence produces an underestimate of the zonal component of the velocity. The consequence of ignoring this process is an apparent reversal of the tracer velocity spiral (compare figure 5 to Jenkins, 1987; figure 14) compared to what is expected from $\beta$-dynamics. Like oxygen, the presence of planetary-scale property gradients plays a significant role in governing $^3$H-$^3$He age distributions.

### 4.4. Subduction Rates

At a single location, the vertical gradient in the $^3$H-$^3$He age might be regarded as a measure of the subduction rate for an isopycnal projected back to its outcrop, once corrected for planetary vorticity gradients (see Jenkins, 1987). However, this approach assumes that the $^3$H-$^3$He age profile represents the true "advective age" of the isopycnal surfaces. The $^3$H-$^3$He age may unfortunately be influenced by mixing processes which in general conspire to lower the apparent age, thereby reducing the vertical age gradient and inflating the apparent subduction rate. This is particularly important because the bias is integrated over the trajectory of fluid parcels. On the shallowest surfaces, where the age tendency term $\tau_t$ is smallest and the extrapolated distance is shortest, this is likely not a severe problem, so such an approach is undoubtedly sound. Going downward into the water column, however, we are on less firm footing. Figure 8 (left panel) shows a plot of the inverse age gradient (*i.e.*, $1/\tau_z$).

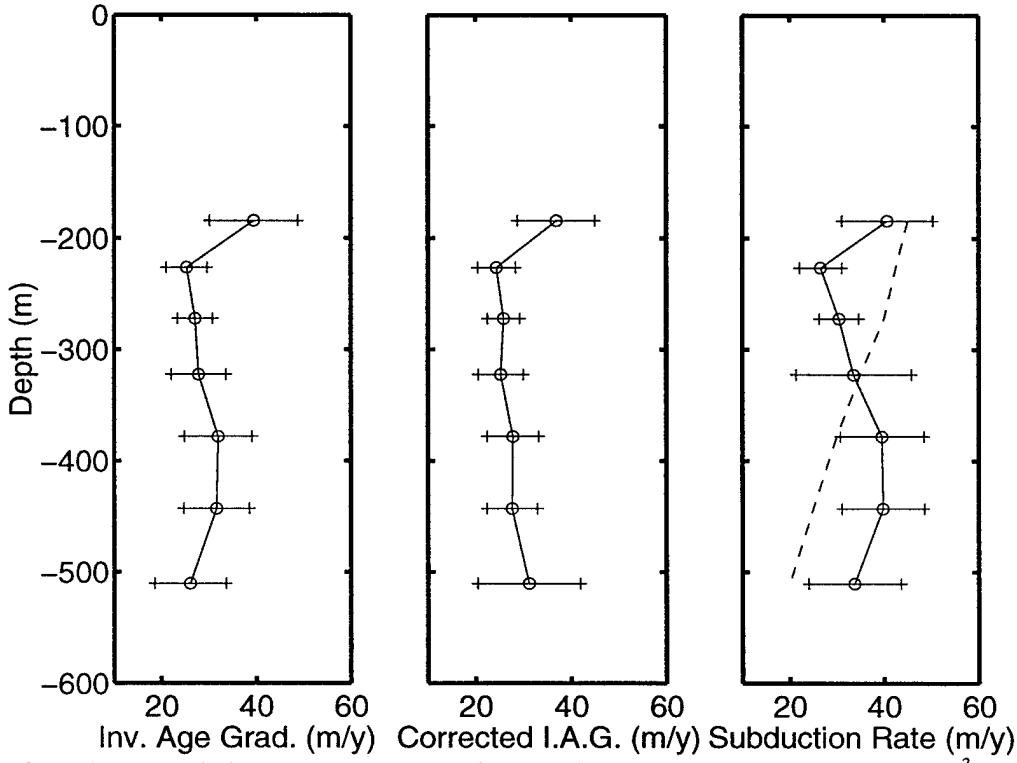


Figure 8: The inverse vertical age gradient (left panel) for pairs of isopycnals between 26.4 and 27.1 kg/m$^3$. The inverse vertical gradient in the corrected age (corrected using date from figure 9) is shown in the center panel. The right panel shows the subduction rate computed from the inverse vertical corrected age gradient and the degree of vortex stretching expected for movement from the climatological winter outcrop position of the isopycnal to the center of the survey region.

I obtained an estimate of the degree to which the $^3$H-$^3$He age is representative of the advective age by running a one-dimensional pipe model for a variety of velocities and a fixed diffusivity of 1000 m$^2$/s.It may be argued that this is an oversimplification of the actual situation, but I would argue that it captures the essence of the tracer behavior sufficiently well to make small corrections. The model was run to two points in time (1979 and 1992) and the advective age (defined as the distance along the pipe divided by the velocity)

contoured as a function of velocity and $^3H$-$^3He$ age. The results are shown in figure 9. Also shown is the locus of $^3H$-$^3He$ age *vs.* velocity for the subduction central point. What is immediately apparent is that the Subduction Area 1992 $^3H$-$^3He$ age data are in fact a good representation of the advective ages. The $^3H$-$^3He$ age actually overestimates the advective age slightly, indicative of a small overshoot in the $^3H$-$^3He$ age non-linear terms. I then apply a correction to the $^3H$-$^3He$ age data by using the model results to estimate the corrected inverse vertical age gradient (shown in figure 8, center panel). Finally, to compute the isopycnal subduction velocities, I further correct the inverse vertical age gradient for vortex stretching associated with movement from the climatological winter outcrop latitude to the current location. This is shown in figure 8 also (right panel), along with estimated ekman pumping rates using annual averaged data of Hellerman and Rosenstien (1983) at the winter outcrop position of the isopycnal.

Near the surface, the ekman pumping rate and the subduction velocity estimates agree within errors, as would be expected. While the ekman pumping rate decreases with depth due to the increasingly more northerly outcrop position (the wind stress curl decreases northward), the subduction velocity remains essentially constant. The difference between these two curves may be regarded as a measure of the buoyancy forced subduction, which would be expected to increase northward, and hence on deeper isopycnals, due to the geography of the winter mixed layer depths (see the arguments contained in Jenkins, 1987). The magnitude of the buoyancy forced subduction rate required, however, is much less than that estimated from the β-triangle data, being of the same order as the ekman pumping rates.

Revisiting the subduction velocity estimates made with the 1979 data (Jenkins, 1987) I must conclude that the deeper $^3H$-$^3He$ age data must substantially overestimate the true rate. This can be seen from figure 9 (left panel), particularly in the low velocity, high age portion of the diagram. Considering the large magnitude of the possible corrections, it is unwise to attempt to make a quantitative statement regarding the β-triangle data, but crude calculations indicate that the corrections indicated bring the estimates to within errors of the Subduction Area values computed here. Thus the large disparity between the apparent subduction rates and ekman pumping reported earlier (Jenkins, 1987) is mostly an artifact of the non-linear behavior of the $^3H$-$^3He$ age during the early part of the tritium invasion. In 1992, however, the tritium and $^3H$-$^3He$ age distributions have now reached a more steady, simpler state.

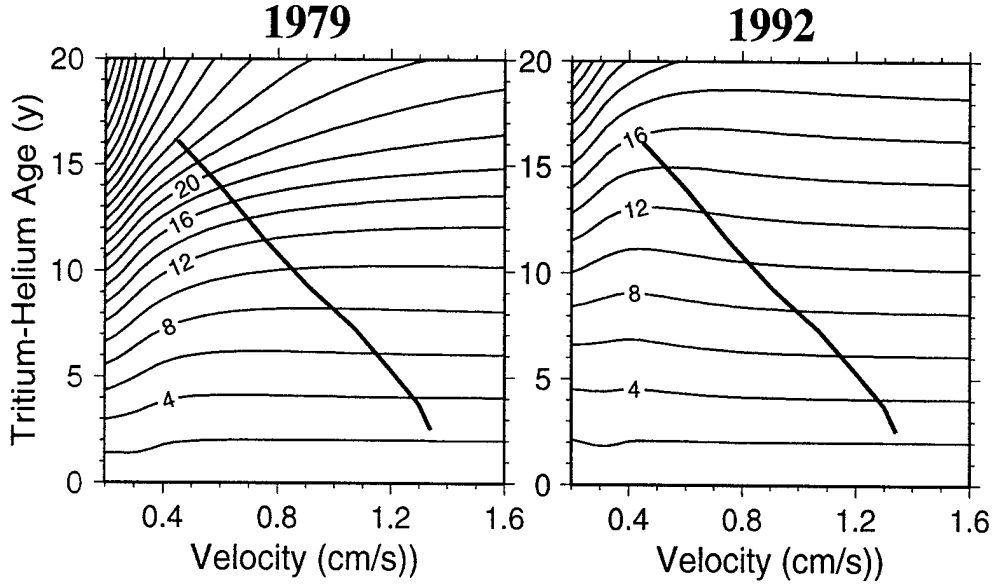


Figure 9: Contours of advective age as a function of velocity and $^3H$-$^3He$ age computed from a pipe model for two times. The solid line marks the mean profile $^3H$-$^3He$ age *vs.* velocity from the subduction region.

## 5. Summary and Conclusions

Consideration of a simple two dimensional gyre model suggests that one can divide the gyre into two regimes: one advectively ventilated, which has streamlines with outcrop, and one which is mixing dominated, where streamlines are all closed. Invasion of tracer into the indirectly ventilated part of the gyre must be accomplished by cross-streamline mixing. Thus one expects very diffusive, low Peclet number behavior of tracers within that part of the main thermocline. In the directly ventilated portion of the gyre, the $^3$H-$^3$He age behaves more as an advective age, especially in the shallower layers. One's approach to studying tracer distributions must be tuned to the area of study.

In the eastern subtropical North Atlantic, an area characterized by direct subduction and ventilation, I combined $^3$H-$^3$He age and other tracer data with geostrophy to calculate isopycnal diffusivities, oxygen consumption rates and absolute velocities. The reference level velocities were determined to an accuracy of better than 1 mm/s. The depth structure of the vertical velocities are consistent with vorticity conservation and extrapolates to local ekman pumping velocities at the surface. The $^3$H-$^3$He age equations dominated the determination of the reference level velocity, while the isopycnal diffusivity was largely determined by the salinity equations. The isopycnal diffusivity is approximately 1200 $m^2/s$ at 300m depth, decreasing weakly downward. The diffusivity also decreases toward the surface, a result which is not intuitive, and which may be an artifact of the increasing importance of unsteady or diapycnal terms on the shallowest surfaces. The oxygen equations add no information except in determining oxygen consumption rates. Oxygen consumption rates can be integrated vertically to obtain a net water column oxygen demand of $4.1\pm0.8 mol(O_2)/m^2/y$, equivalent to an export production of $2.5\pm0.5$ $mol/m^2/y$ carbon.

Subduction rate as a function of density horizon can be estimated from the vertical gradient in $^3$H-$^3$He age, provided that it is a measure of advective age. This assumption is valid on the shallowest surfaces, but requires a small model-dependent correction on the deeper horizons. The subduction velocities thus determined agree with ekman pumping rates near the surface, but do not decrease with depth like the isopycnic projected ekman pumping velocities. The difference signals the increasing importance of buoyancy forced subduction for deeper isopycnals. The earlier $\beta$-triangle estimates were clearly biased in the deeper waters with the non-linear age effect, which was stronger at that time. The magnitude of the bias is estimated to be sufficient to bring the $\beta$-triangle results into agreement with the estimates made here.

The hope is that this paper demonstrates the utility and value of transient tracer measurements in studying thermocline ventilation and circulation. My thesis is that the $^3$H-$^3$He age and its complement $\zeta$ provide powerful constraints on mixing rates and velocities in the subtropical North Atlantic. One of the keys to this success is combining the transient tracer observations with other sources of information. Another is the acquisition of appropriate data sets. Clearly time series measurements are of considerable value in documenting the passage of these tracers into the ocean. As important are fully three dimensional surveys of property distributions to fully diagnose all aspects of mixing and circulation. It is extraordinarily difficult (if not impossible) to extract this kind of information from sparsely spaced sections. Experience dictates that gridded surveys are necessary if we are to obtain realistic estimates of oxygen consumption rates. The work done here suggests that this approach can be successfully applied in other subtropical gyres.

## 6. Publications Resulting from this Program


Joyce, T.M. and W.J. Jenkins (1993) Spatial variability of subducting water in the North Atlantic: a pilot study. *J. Geophys. Res.* **98** 10111-10124.

Jenkins, W.J. (1996) Ventilation of the North Atlantic thermocline. *EOS Trans. AGU* **76**, OS12K-2

Jenkins, W. J. (1996) Using Transient Tracers in a WOCE Process Study: Tritium-3He Dating in the Subduction Experiment. *U.S. WOCE Newsletter* **8**,

Robbins, P.E., and W.J. Jenkins (1996) Temporal evolution of the tritium-$^3$He age field in the North Atlantic subtropical thermocline. *EOS Tran. AGU* **77**, 355.

Jenkins, W. J. (1997) Studying thermocline ventilation and circulation using tritium and $^3$He. *J. Geophys. Res.* In Press.


## 7. References

Armi, L. and H. Stommel, Four views of a portion of the North Atlantic subtropical gyre. *J. Phys. Oceanogr.* 13, 828-857, 1983.

Clarke, W.B., W. J. Jenkins and Z. Top, Determination of tritium by mass-spectrometric measurement of $^{3}$He. *Int. J. App. Rad. Isotopes* 27, 512-522, 1976.

Doney, S. C., and W. J. Jenkins, The effect of boundary conditions on tracer estimates of thermocline ventilation rates. *J. Mar. Res.* 46, 947-965, 1988.

Doney, S. C., W. J. Jenkins and H.G. Ostlund, A tritium budget for the North Atlantic. *J. Geophys. Res.* 98, 18069-18081, 1993.

Doney, S. C. and W. J Jenkins, Ventilation of the deep western boundary current and abyssal western North Atlantic: Estimates from tritium and $^{3}$He distributions. *J. Phys. Oceanogr.* 24, 638-659, 1994.

Dreisigacker, E., and W. Roether, Tritium and $^{90}$Sr in North Atlantic surface water. *Earth Planet. Sci. Lett.*38, 301-312, 1979.

Hellerman, S. and M. Rosenstein, Normal monthly wind stress over the world ocean with error estimates. *J. Phys. Oceanogr.* 13, 1093-1104, 1983.

Hogg, N., A least-squares fit of the advective-diffusive equations to Levitus Atlas data. *J. Mar. Res.* 45, 347-375, 1987.

Isemer, H J. and L. Hasse, *The Bunker Climate Atlas of the North Atlantic Ocean,* Vol. 2. *Air-Sea Interactions.* 256pp. Springer-Verlag, 1987.

Lott, D. E. and W. J. Jenkins, An automated cryogenic charcoal trap system for helium isotope mass spectrometry. *Rev. Sci. Instrum.* 55, 1982-1988, 1984.Jenkins, W. J., Tritium and $^{3}$He in the Sargasso Sea. *J. Mar. Res.* 38, 533-569, 1980.

Jenkins, W. J., On the climate of a subtropical ocean gyre: decade time scale variations in water mass renewal in the Sargasso Sea *J. Mar. Res.* 40(S), 265-290, 1982a.

Jenkins, W J., Oxygen utilization rates in the North Atlantic subtropical gyre and primary production in oligotrophic systems. *NATURE* 300, 246-249, 1982b.

Jenkins, W. J., $^{3}$H and $^{3}$He in the Beta Triangle: observations of gyre ventilation and oxygen utilization rates. *J. Phys. Oceanogr.* 17, 763-783, 1987.

Jenkins, W. J., Nitrate flux into the euphotic zone near Bermuda. *Nature* 331, 521-523, 1988.

Jenkins, W. J., The use of anthropogenic tritium and helium-3 to study subtropical ventilation and circulation. *Phil. Trans. Royal Soc.* (London) A 325, 43-61, 1988.

Jenkins, W. J., Determination of isopycnal diffusivity in the Sargasso Sea. *J. Phys. Oceanogr.* 21, 1058-1061, 1991.

Jenkins, W. J. and Goldman, J. C., Seasonal oxygen cycling and primary production in the Sargasso Sea. *J. Mar. Res.* 43, 465-491, 1985.

Jenkins, W .J. and D. W. R. Wallace, Tracer based inferences of new primary production in the sea. *In Primary Production and Biogeochemical Cycles in the Sea.* P. G. Falkowski and A. D. Woodhead (Ed.) Plenum Press, 299-316, 1992.

Joyce, T. M. and W. J. Jenkins, Spatial variability of subducting water in the North Atlantic: a pilot study. *J. Geophys. Res.* 98, 10111-10124, 1993.

Ledwell, J. R., A. J. Watson, and C. S. Law, Evidence for slow mixing across the pycnocline from and open ocean tracer release experiment. *Nature* 364, 701-703, 1993.

Levitus, S., World Ocean Atlas, 1994. CD-ROM Data Sets. NOAA/NODC Ocean Climate Laboratory, 1994.

Mayer, D. A. and R.H. Weisberg, A description of the COADS surface meteorological fields and the implied Sverdrup transports for the Atlantic Ocean from 30(S to 60(N. *J. Phys. Oceanogr.* 23, 2201-2221, 1993.

Muller, T. J. and G. Siedler, Multi-year current time series in the eastern North Atlantic Ocean. *J. Mar. Res.* 50, 63-98, 1992.

Olbers, D. J., M. Wenzel and J. Willebrand, The inference of North Atlantic circulation patterns from climatological hydrographic data. *Rev Geophys.* 23, 313-356, 1985.

Qiu, B. and R. X. Huang, Ventilation of the North Atlantic and North Pacific: subduction *vs.* obduction. *J. Phys. Oceanogr.* 25, 2374-2390, 1995.

Takahashi, T. T., W. S. Broecker, and S. Langer, Redfield ratio based on chemical data from isopycnal surfaces. *J. Geophys. Res.* 90, 6907-6926, 1985.

Thiele, G. and J. L. Sarmiento, Tracer dating and ocean ventilation. *J. Geophys. Res.* 95, 9377-9391, 1990.

Worthington, L. V., On the North Atlantic Ciculation. 110pp, *The Johns Hopkins Oceanographic Studies* 6, 1976.

Zhang, H-M., and N. G. Hogg, Circulation and water mass balance in the Brazil Basin. *J. Mar. Res.* 50, 385-420, 1992.